HARMONIC NONLINEAR ANALYSIS OF THREE-PHASE FOUR-WIRE DISTRIBUTION NETWORKS

Lieven DEGROOTE
Ghent University - Belgium
Lieven.Degroote@UGent.be

Bert RENDERS
Ghent University - Belgium
Bert.Renders@UGent.be

Bart MEERSMAN
Ghent University - Belgium
Bart.Meersman@UGent.be

Lieven VANDEVELDE
Ghent University - Belgium
Lieven.Vandevelde@UGent.be

ABSTRACT

In this paper a solution method for the harmonic analysis of three-phase four-wire distribution networks is presented. In order to obtain a more accurate model of a real distribution network a nonlinear transformer model has been developed. The construction of the transformer model and the implementation in a load flow program will be discussed. The nonlinear loads in the network will be simulated in the time domain. The total harmonic distortion (THD) of the voltage in the distribution network will be compared to the situation where the nonlinear loads are replaced by constant harmonic current sources. This way, the effects of attenuation and diversity on the voltage THD will be explained. The effects of different system parameters on the voltage THD will also be investigated.

INTRODUCTION

Because of the increasing presence of harmonic producing equipment, harmonic load-flow simulations are an important component of power system analysis and design [1–4]. It is well known that the harmonic currents drawn by the loads are dependent of the supply voltage, except for cases where the nonlinear loads are replaced with constant current injections.
The model described in the paper uses the magnetic equivalent circuit (MEC) of a transformer implemented in symmetrical components. This type of spatial discretisation yields a good representation of the physical shape of the transformer just like the FE method although it is not as detailed as the finite element (FE) method and thus significantly faster. The utilized model has the benefit that the saturation of the yokes is considered as compared to the representation of the nonlinear inductance (e.g. [5]). The model presented here allows representing coupling between the phases and different saturation levels of every phase can be taken into account.
For the time discretisation, the harmonic balance method is used, this implies that a fast fourier transform (FFT) is performed on the reluctance in the different parts of the transformer. For the three-phase transformer this also implies that the reluctance has both a time and a space harmonic order. So the calculation method presented here has been developed in the (frequency, spatial order) domain, analogously to the analysis of the magnetic fields in squirrel-cage induction motors, presented in [6]. For all quantities (current, voltage, flux, magnetic reluctivity), the temporal and spatial variation is resolved into components characterised by frequency, order and complex value. In the case of three-phase transformers the spatial orders correspond to the symmetrical components. An advantage of this method is a better understanding in the interaction between different harmonics. Another advantage is that less fast fourier transformations are needed as mentioned in [7]. The harmonic balance method allows the user to choose the number of harmonics that determine the saturation state. This allows to obtain a good estimation of the saturation state. The other harmonics are linearised around this working point.
In this paper the case of a distribution network with two feeders will be investigated. The influence of nonlinear loads on this distribution network is verified by replacing them by constant current sources. The nonlinear loads are simulated in the time domain in every iteration. The effects of attenuation and diversity on the voltage THD will be explained. The effect of different system parameters on the THD will be investigated. The influence of the transformer model on the voltage THD will also be elaborated.

DISTRIBUTION NETWORK MODEL

Model Description of the Distribution Network

The model of the distribution network is a three phase network implemented in symmetrical components. It consists of a HV/MV transformer, connected to several MV/LV transformers. The number of MV/LV transformers can be varied. The MV/LV transformers supply different feeders, for every transformer the number of feeders is free. The length, type and consumed power of every feeder can also be enforced by the user. The distribution model can contain different nonlinear loads, that can be placed in specific nodes.

Solution Method

The model is solved with a hybrid method. This implies that a part of the network is implemented in the frequency domain and the other part is simulated in the time domain. The line elements and the linear loads are simulated in the frequency domain, the nonlinear loads in the time domain (e.g. by using Plecs®, a Matlab® toolbox). The output data of this part (e.g. the currents) can be transformed to the frequency domain by performing a fast fourier transform (FFT) on the steady state current of the nonlinear load. For all calculations the first 40 harmonics are considered.
The model is solved with the iterative forward-backward method. This method consists of two steps, the backward and the forward sweep respectively. In the backward sweep, the voltage is calculated in every node, starting from the source and taking into consideration the voltage drop in every line section. In the first step, the voltage spectrum of the HV-bus, which is considered to be constant, is used in every node. Then the harmonic current drawn by every load is calculated. In the forward sweep, the harmonic current through every branch is calculated. This iterative method continues until convergence is achieved.

The use of an iterative method may lead to some convergence problems. Sometimes the method becomes numerically unstable. The reason for this instability is the proportion of the load impedance to the impedance between the considered node and the HV-bus. A possible solution for this problem, without changing the physical properties of the network, is inserting a reactance pair [8]. To solve the network with the iterative method the voltage spectrum in the fictitious node between each reactance pair is considered. So the impedance of the load, seen from these fictitious nodes, is larger and the impedance between these fictitious nodes and the HV-bus is smaller.

THE NONLINEAR TRANSFORMER MODEL

In this section a model for a three-phase, three-legged transformer is analysed.
In the following equations, straight indices indicate a space harmonic and slanted indices denote a time harmonic.

Electric and Magnetic Transformer Equations

In Fig. 1 the equivalent electric and magnetic circuit of a three-phase three-legged transformer is shown. Here is assumed that the direct and inverse component of the flux closes through the yokes and that only the homopolar part of the flux closes via the air, which results in Fig. 1 (b) for the direct and inverse component and Fig. 1 (c) for the homopolar component.
The electrical equations derived from Fig. 1(a) are

$$\begin{aligned} U_{\mathrm{pn}} &= R_{\mathrm{p}} I_{\mathrm{pn}} + L_{\mathrm{p}\sigma}\frac{dI_{\mathrm{pn}}}{dt} + N_{\mathrm{p}}\frac{d\Phi_{\mathrm{n}}}{dt} \\ U^{'}_{\mathrm{sn}} &= R^{'}_{\mathrm{s}} I^{'}_{\mathrm{sn}} + L^{'}_{\mathrm{s}\sigma}\frac{dI^{'}_{\mathrm{sn}}}{dt} + N_{\mathrm{p}}\frac{d\Phi_{\mathrm{n}}}{dt} \quad (\mathrm{n} = \mathrm{a},\mathrm{b},\mathrm{c}) \end{aligned} \tag{1}$$

with

- $I_{\mathrm{pn}}, I^{'}_{\mathrm{sn}}, U_{\mathrm{pn}}, U^{'}_{\mathrm{sn}}$: the currents and the voltages of the primary and the secondary windings referred to the primary side
- Φ_{n}: the core magnetic flux
- $R_{\mathrm{p}}, R^{'}_{\mathrm{s}}, L_{\mathrm{p}\sigma}, L^{'}_{\mathrm{s}\sigma}$: the winding resistances and the constant leakage inductances referred to the primary side
- $N_{\mathrm{p}}, N_{\mathrm{s}}$: the number of turns

The relations between the magnetic flux and the currents obtained from this circuit are

$$\begin{aligned} 0 &= N_{\mathrm{p}}(I_{\mathrm{pa}} + I^{'}_{\mathrm{sa}}) - N_{\mathrm{p}}(I_{\mathrm{pb}} + I^{'}_{\mathrm{sb}}) \\ &\quad - (\mathcal{R}_{\mathrm{a}} + \frac{2}{3}\mathcal{R}_{\mathrm{ab}})\Phi_{\mathrm{a}} + (\mathcal{R}_{\mathrm{b}} + \frac{1}{3}\mathcal{R}_{\mathrm{ab}})\Phi_{\mathrm{b}} + \frac{\mathcal{R}_{\mathrm{ab}}}{3}\Phi_{\mathrm{c}} \\ 0 &= N_{\mathrm{p}}(I_{\mathrm{pc}} + I^{'}_{\mathrm{sc}}) - N_{\mathrm{p}}(I_{\mathrm{pb}} + I^{'}_{\mathrm{sb}}) \\ &\quad - (\mathcal{R}_{\mathrm{c}} + \frac{2}{3}\mathcal{R}_{\mathrm{bc}})\Phi_{\mathrm{c}} + (\mathcal{R}_{\mathrm{b}} + \frac{1}{3}\mathcal{R}_{\mathrm{bc}})\Phi_{\mathrm{b}} + \frac{\mathcal{R}_{\mathrm{bc}}}{3}\Phi_{\mathrm{a}} \\ 0 &= \sum_{\mathrm{n=a,b,c}} N_{\mathrm{p}}(I_{\mathrm{pn}} + I^{'}_{\mathrm{sn}}) - \sum_{\mathrm{n=a,b,c}} (\mathcal{R}_{\mathrm{n}} + 3\mathcal{R}_{\mathrm{d}})\Phi_{\mathrm{n}} \end{aligned} \tag{2}$$

where $\mathcal{R}_{\mathrm{n}}$ is the nonlinear reluctance of leg n, $\mathcal{R}_{\mathrm{ab}}$ and $\mathcal{R}_{\mathrm{bc}}$ are the nonlinear reluctances of the yoke between two legs and $3\mathcal{R}_{\mathrm{d}}$ is the constant reluctance of the air branch.

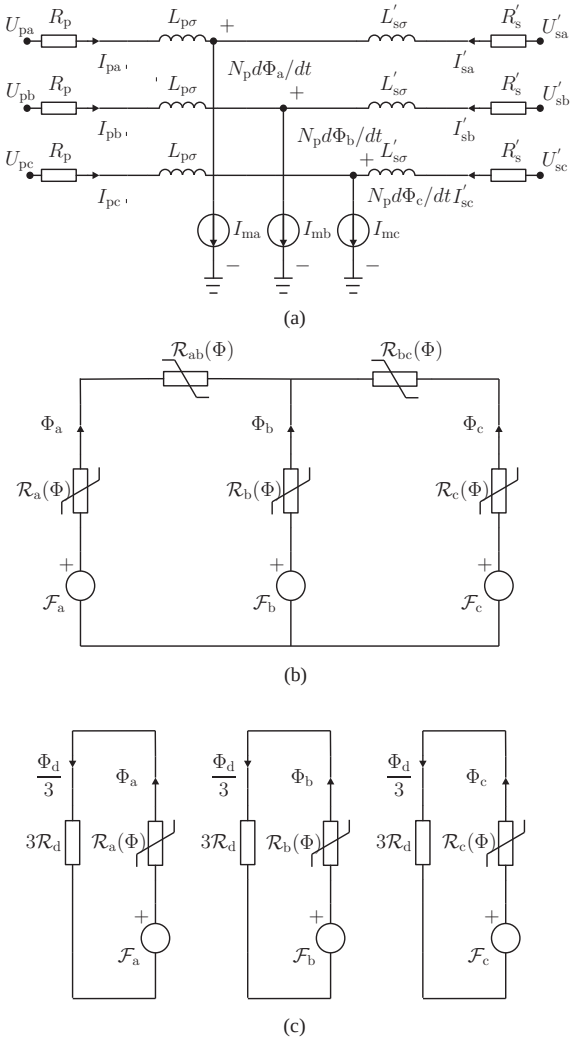

Figure 1: Equivalent electric (a) and magnetic circuits of a three-phase three-legged transformer, for the direct and inverse component (b) and for the homopolar component (c).

Equations (1) and (2) can be transformed into symmetrical components, which gives the next equations in the frequency domain (with k the harmonic order) for the electrical part.

$$\begin{aligned} \underline{U}_{\mathrm{pn}k} &= \underline{\underline{Z}}_{\mathrm{pn}k}\underline{I}_{\mathrm{pn}k} + j\omega_k N_{\mathrm{p}}\underline{\Phi}_{\mathrm{n}k} \\ \underline{U}^{'}_{\mathrm{sn}k} &= \underline{\underline{Z}}^{'}_{\mathrm{sn}k}\underline{I}^{'}_{\mathrm{sn}k} + j\omega_k N_{\mathrm{p}}\underline{\Phi}_{\mathrm{n}k} \quad (\mathrm{n} = 0,1,2) \end{aligned} \tag{3}$$

In these equations the double underlined symbols are tensors, which correspond to 2×2 matrices. The single underlined symbols are complex values but they are applied as 2×1 column matrices.
For the magnetic part, the equations would be uncoupled if the reluctances of the yokes would not be taken into account. The multiplication of a reluctance, with space harmonic order n and time harmonic order k, and a flux, with space harmonic order m and time harmonic order l, leads to a magneto motive force (mmf) with time harmonic order h and space harmonic order κ. A first contribution is

$$h = k + l; \qquad \kappa = \mathrm{m} + \mathrm{n} + 3\mathrm{q}$$

and the second one is

$$h = k - l; \qquad \kappa = \mathrm{m} - \mathrm{n} + 3\mathrm{q}$$

if $k > l$ and else

$$h = l - k; \qquad \kappa = \mathrm{n} - \mathrm{m} + 3\mathrm{q}$$

In the above equations, q has to be -1, 0 or 1 in order to obtain a value for κ that equals 0, 1 or 2.
To obtain the influence of the yoke reluctances, equation (2) has to be considered. By using some basic calculus this equation can be rewritten as

$$\begin{aligned} 0 = &-N_{\mathrm{p}}(\underline{I}_{\mathrm{p0}} + \underline{I}'_{\mathrm{s0}}) + (\frac{\underline{\mathcal{R}}_{\mathrm{a}} + \underline{\mathcal{R}}_{\mathrm{b}} + \underline{\mathcal{R}}_{\mathrm{c}}}{3} + 3\underline{\mathcal{R}}_{\mathrm{d}})\underline{\Phi}_0 \\ &+ (\frac{\underline{\mathcal{R}}_{\mathrm{a}} + \underline{\mathcal{R}}_{\mathrm{b}}\underline{a}^2 + \underline{\mathcal{R}}_{\mathrm{c}}\underline{a}}{3})\underline{\Phi}_1 \\ &+ (\frac{\underline{\mathcal{R}}_{\mathrm{a}} + \underline{\mathcal{R}}_{\mathrm{b}}\underline{a} + \underline{\mathcal{R}}_{\mathrm{c}}\underline{a}^2}{3})\underline{\Phi}_2 \end{aligned}$$

$$\begin{aligned} 0 = &-N_{\mathrm{p}}(\underline{I}_{\mathrm{p1}} + \underline{I}'_{\mathrm{s1}}) + (\frac{\underline{\mathcal{R}}_{\mathrm{a}} + \underline{a}\underline{\mathcal{R}}_{\mathrm{b}} + \underline{a}^2\underline{\mathcal{R}}_{\mathrm{c}}}{3})\underline{\Phi}_0 \\ &+ (\frac{\underline{\mathcal{R}}_{\mathrm{a}} + \underline{a}\underline{\mathcal{R}}_{\mathrm{b}}\underline{a}^2 + \underline{a}^2\underline{\mathcal{R}}_{\mathrm{c}}\underline{a}}{3} + \frac{\underline{\mathcal{R}}_{\mathrm{ab}} + \underline{a}^2\underline{\mathcal{R}}_{\mathrm{bc}}\underline{a}}{3})\underline{\Phi}_1 \\ &+ (\frac{\underline{\mathcal{R}}_{\mathrm{a}} + \underline{a}\underline{\mathcal{R}}_{\mathrm{b}}\underline{a} + \underline{a}^2\underline{\mathcal{R}}_{\mathrm{c}}\underline{a}^2}{3} + \frac{\underline{\mathcal{R}}_{\mathrm{ab}} + \underline{a}^2\underline{\mathcal{R}}_{\mathrm{bc}}\underline{a}^2}{3})\underline{\Phi}_2 \end{aligned}$$

$$\begin{aligned} 0 = &-N_{\mathrm{p}}(\underline{I}_{\mathrm{p2}} + \underline{I}'_{\mathrm{s2}}) + (\frac{\underline{\mathcal{R}}_{\mathrm{a}} + \underline{a}^2\underline{\mathcal{R}}_{\mathrm{b}} + \underline{a}\underline{\mathcal{R}}_{\mathrm{c}}}{3})\underline{\Phi}_0 \\ &+ (\frac{\underline{\mathcal{R}}_{\mathrm{a}} + \underline{a}^2\underline{\mathcal{R}}_{\mathrm{b}}\underline{a}^2 + \underline{a}\underline{\mathcal{R}}_{\mathrm{c}}\underline{a}}{3} + \frac{\underline{\mathcal{R}}_{\mathrm{ab}} + \underline{a}\underline{\mathcal{R}}_{\mathrm{bc}}\underline{a}}{3})\underline{\Phi}_1 \\ &+ (\frac{\underline{\mathcal{R}}_{\mathrm{a}} + \underline{a}^2\underline{\mathcal{R}}_{\mathrm{b}}\underline{a} + \underline{a}\underline{\mathcal{R}}_{\mathrm{c}}\underline{a}^2}{3} + \frac{\underline{\mathcal{R}}_{\mathrm{ab}} + \underline{a}\underline{\mathcal{R}}_{\mathrm{bc}}\underline{a}^2}{3})\underline{\Phi}_2 \end{aligned}$$

where $\underline{a}$ yields a phase angle rotation of $120°$.
Depending on the time harmonic order of the reluctance and the flux, these equations can be rewritten in symmetrical components of the reluctances $\underline{\mathcal{R}}_{\mathrm{a}}$, $\underline{\mathcal{R}}_{\mathrm{b}}$ and $\underline{\mathcal{R}}_{\mathrm{c}}$.
This equation and (3) are nonlinear equations of the form

$$G(x) = S(x)x - b = 0 \tag{4}$$

The components of the state vector x are the harmonic currents, $\underline{I}_{\mathrm{p}k}$ and $\underline{I}'_{\mathrm{s}k}$, and the flux $\underline{\Phi}_k$. The vector b consists of the voltages, $\underline{U}_{\mathrm{p}k}$ and $\underline{U}'_{\mathrm{s}k}$, and the magnetic potential.
Equation (4) will be solved in two steps. In the first step only the first six odd harmonics are considered to determine the global saturation state ($k = 1, 3, 5, 7, 9, 11$). In this step the Newton-Raphson method is used, which consists of the iterative application of the algorithm:

$$x^{m+1} = x^m - DG(x^m)^{-1}G(x^m) \tag{5}$$

The iterative process continues until convergence is reached. The calculation of the Jacobian $DG(x)$ is obtained numerically as $DG(x) = S + (\partial S/\partial x) \cdot x$ due to the particular form of the nonlinear equation $G(x) = S(x)x - b = 0$.
In the second step, the first forty harmonics are considered ($k = 1, ..., 40$). The model is linearised by using the differential reluctances and the magnetic current is determined by solving the following equation:

$$x = P^{-1}b \tag{6}$$

The matrix P is obtained in the same way as S. But the reluctance components are replaced by the differential reluctances for the cases where the flux harmonic order does not equal one of the first six odd harmonics.

CASE STUDY

In this case study the network depicted in Fig. 2 will be elaborated on. The network consists of two feeders with 10 nodes each where equally distributed loads consume 30kVA in total with a power factor of 0.8. Different simulations will be performed on this network in order to investigate the attenuation and the diversity effect. Therefore, four peak rectifiers are placed on the network and each of the rectifiers supplies a load that absorbs 10kVA.

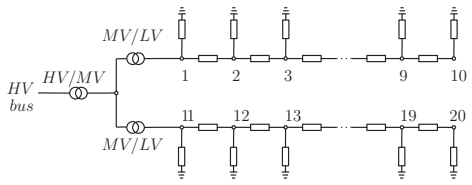

Figure 2: Topology of the considered distribution network.

Attenuation Effect

When nonlinear loads are replaced by a fixed harmonic current source, there will be an error on the voltage THD when compared to the simulation where the currents are dependent on the node voltage.
For this simulation, four single phase peak rectifiers are connected to feeder 1 in node 2, 4, 6 and 8 of phase a. The difference in the voltage THD in every node can be found in Fig. 3. When comparing the first bar with the second bar, one can see that the voltage THD is lower when the current drawn by the nonlinear load is dependent on the node voltage. This can be explained by considering the attenuation factor:

$$AF_h = \frac{I_h^N}{NI_h} \tag{7}$$

with

- I_h^N: Resultant current for harmonic h for N units.

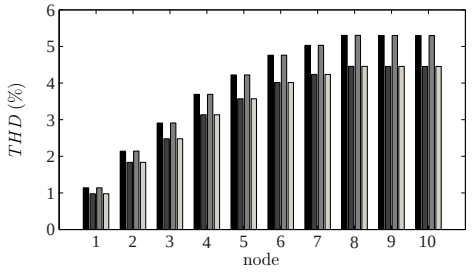

Figure 3: The voltage THD in the nodes 1 to 10 of phase a. The first bars (black ones) represent the case where the nonlinear load is a fixed harmonic current source. The second bars where the load current is dependent on the node voltage. The two last bars are the same as the first ones but here the magnetizing current has not been considered during the simulation

- I_h: Current of harmonic h when the nonlinear load is replaced by a fixed harmonic current source.

This factor is given for every odd harmonic in Fig. 4. The factor is generally spoken lower than one which explains the smaller voltage THD for the second bar.

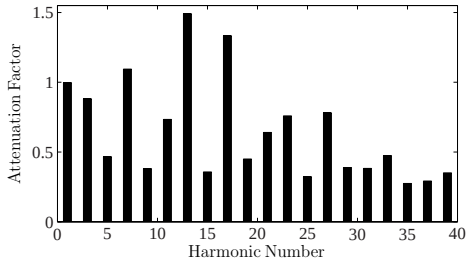

Figure 4: The attenuation factor of the harmonic currents.

The same simulation has been performed without considering the influence of the magnetizing current in every iteration. The results are added in Fig. 3. The conclusion that can be drawn is that the voltage THD is slightly higher if the magnetizing currents are considered.

Diversity Effect

The diversity effect describes possible harmonic cancellation between nonlinear loads. A possible origin can be found in the variation of the line impedance magnitude or the different X/R ratios of the line impedance. To demonstrate this effect a simulation has been performed in which feeder 1 of the distribution network of Fig. 2 is implemented as a line and feeder 2 has the physical properties of a cable. In this case the two feeders have a different X/R ratio. The four nonlinear nodes are placed on phase a in the nodes 4, 8, 14 and 18. The influence of the line impedance magnitude can be considered when comparing the harmonic cancellation of the rectifiers in node 4 and 14 with the harmonic cancellation of those in 8 and 18.
In order to quantify the effect of the phase angle dispersion, the following current harmonics diversity factor has been defined:

$$DF_h = \left| \frac{\sum_{i=1}^{N} I_h^i}{\sum_{i=1}^{N} \left| I_h^i \right|} \right| \tag{8}$$

where:

- N is the considered amount of nonlinear nodes.
- $I_h^I = \left| I_h^i \right| \angle \theta_h^i$ is the harmonic current of order h injected by the i-th load of the N considered loads.

In Fig. 5 the diversity factor of the nonlinear loads in 4 and 14 is plotted in the first bar and in the second bar the diversity factor of the rectifiers in node 8 and 18 is displayed.
The diversity factor ranges between 0 and 1. A small value implies a significant amount of cancellation due to the circulation of harmonic currents among individual loads. From Fig. 5 one can also deduce that a higher line impedance magnitude results in smaller diversity factors.

CONCLUSION

In this paper the construction of a simulation model for realistic distribution networks has been set up. This model has been used for case studies in which the nonlinear loads

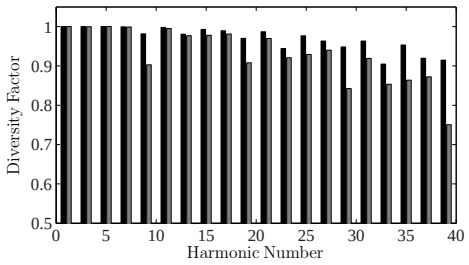

Figure 5: The diversity factor of the rectifiers in node 4 and 14 (black) and of the rectifiers in node 8 and 18 (grey).

can be presented by fixed current sources or by voltage dependent harmonic current sources. Due to the representation of the the nonlinear loads with fixed current sources an overestimation of the voltage THD was obtained. The reason for this overestimation has been explained with the attenuation and the diversity effect.

REFERENCES

[1] IEEE Task Force on Harmonics Modeling and Simulation, 1996, "Modeling and simulation of the propagation of harmonics in electric power networks. Part I: Concepts, models, and simulation techniques," *IEEE Trans. Power Delivery*, vol. 11, no. 1, 452–474.

[2] A. Semleyn and A. Medina, 1995, "Computation of the periodic steady state in systems with nonlinear components using a hybrid time and frequency domain methodology," *IEEE Trans. Power Syst.*, vol. 10, no. 1, 1498–1504.

[3] J. Ghijselen, W. Ryckaert, and J. Melkebeek, 2004, "Influence of electric power distribution system design on harmonic propagation," *Electrical Engineering*, vol. 86, 181–190.

[4] A. Mansoor, W. Grady, A. Chowdhury, and M. Samotyj, 1995, "An investigation of harmonic attenuation and diversity among single-phase power electronic loads," *IEEE Trans. Power Delivery*, vol. 10, no. 1, 467–473.

[5] H. W. Dommel, A. Yan, and S. Wei, 1986, "Harmonics from transformer saturation," *IEEE Trans. Power Delivery*, vol. 1, no. 2, 209–215.

[6] L. Vandevelde and J. Melkebeek, 2001, "Numerical analysis of vibrations of squirrel-cage induction motors based on magnetic equivalent circuits and structural finite element models," in *Conference Record of the IEEE 36th IAS Annual Meeting. (IAS'01)*, vol. 4, 2288–2295.

[7] A. Semlyen, E. Acha, and J. Arrillaga, 1987, "Harmonic Norton equivalent for the magnetizing branch of a transformer," in *Proc. Inst. Elect. Eng. C*, vol. 134, 162–169.

[8] R. Carbone, M. Fantauzzi, F. Gagliardi, and A. Testa, 1993 "Some considerations on the iterative harmonic analysis convergence," *IEEE Trans. Power Delivery*, vol. 8, no. 2, 487–495.